MASTER COPY KEEP THIS COPY FOR REPRODUCTION PURPOSES

REPORT DOCUMENTATION PAGE

Form Approved
OMB No. 0704-0188

1. AGENCY USE ONLY (Leave blank)	2. REPORT DATE	3. REPORT TYPE AND DATES COVERED
	8 OCT 1999	Final: 18 DEC 1998 - 18 JULY 1999

4. TITLE AND SUBTITLE

Quantum Dot Array Formation through Biomolecular Nanopatterning

5. FUNDING NUMBERS

$69,976.

DAAD19-99-C-0019

6. AUTHOR(S)

H.P. Gillis

7. PERFORMING ORGANIZATION NAME(S) AND ADDRESS(ES)

Materials Research Source LLC
2895 Butter Creek Drive
Pasadena, CA 91107-5908

8. PERFORMING ORGANIZATION REPORT NUMBER

9. SPONSORING/MONITORING AGENCY NAME(S) AND ADDRESS(ES)

U.S. Army Research Office
P.O. Box 12211
Research Triangle Park, NC 27709-2211

10. SPONSORING/MONITORING AGENCY REPORT NUMBER

11. SUPPLEMENTARY NOTES

The views, opinions and/or findings contained in this report are those of the author(s) and should not be construed as an official Department of the Army position, policy, or decision, unless so designated by other documentation.

12a. DISTRIBUTION / AVAILABILITY STATEMENT

Approved for public release; distribution unlimited

12b. DISTRIBUTION CODE

13. ABSTRACT *(Maximum 200 words)*

Report developedunder SBIR contract for Topic A98-028: The objective is to demonstrate the feasibility of forming precisely ordered and precisely located arrays of semiconductor quantum dots by using biomolecular templates and Low Energy Electron Enhanced Etching (LE4) to define in a substrate an array of holes with diameters comparable to the size of quantum dots sought, and then growing one quantum dot in each "nano-hole" by self-assembly of deposited adatoms. In Phae I, key methodology was developed: (1) depositing the biomolecular templates on clean (hydrophobic) Si(100) surfaces rather than on oxidized (hydrophilic)surfaces, in oder to simplify the subsequent LE4 process; (2) identifying LE4 process conditions for etching the nano-pattern; (3) stripping the template-generated masks after LE4 by wet chemical methods. Deposition of GaAs by Molecular Beam Epitaxy (MBE) produced quantum dots randomly distributed over the surface, because the mask stripping process oxidizes the etched surface. In Phase I Option, methods for removing this oxide without destroying the etched nano-pattern will be demonstrated. These arrays have potential applications in optical emitters and detectors, single electron transistors, and high-density memory arrays.

14. SUBJECT TERMS

Quantum dot arrays, nanopatterning, LE4, biomolecular templates, S-layers, SBIR report

15. NUMBER OF PAGES

17

16. PRICE CODE

17. SECURITY CLASSIFICATION OF REPORT	18. SECURITY CLASSIFICATION OF THIS PAGE	19. SECURITY CLASSIFICATION OF ABSTRACT	20. LIMITATION OF ABSTRACT
UNCLASSIFIED	UNCLASSIFIED	UNCLASSIFIED	UL

Quantum Dot Array Formation through Biomolecular Nanopatterning

Contract No. DAAD19-99-C-0019
Final Report: 18 DEC 1998 – 18 JULY 1999

1. INTRODUCTION AND BACKGROUND

The long-term goal of this project is to perfect a technology for creating precisely ordered and precisely located arrays of semiconductor quantum dots. The approach we have adopted is to use biomolecular templates to first create in a substrate an array of holes with diameters comparable to the size of quantum dots sought and then fabricate the quantum dots by self-assembly of adatoms deposited on the patterned surface. The severely restricted diffusion field defined by the holes will dominate nucleation and growth to produce a single quantum dot in each etched hole.

This approach is based on previous work,[1] in which we used Low Energy Electron Enhanced Etching (LE4) in a DC hydrogen plasma to transfer the nanometer-scale pattern of the biomolecular template into a Si substrate. Using high resolution cross-sectional transmission electron microscopy (HRXTEM), we determined that we had transferred the biological pattern into the substrate to a depth of 10 nm and that the etching was fairly isotropic. After etching, we removed the mask, intentionally oxidized the surface, and then deposited a thin layer of titanium to produce an ordered array of quantum dots.

As specific steps toward demonstrating the feasibility of our proposed method for forming ordered arrays of semiconductor quantum dots on a substrate, this Phase I project was devoted to refinements in the previous methods. Specifically, we sought increased control over the profile of the etched holes and the uniformity of the etched hole array. And, we sought to deposit semiconductor quantum dots instead of metal dots in the etched array of holes.

2. OBJECTIVES

These goals were sought through the following specific objectives:

2.1. to deposit the biomolecular template directly on (hydrophobic) Si(100) surfaces;

because the biomolecular masks have been traditionally applied to the substrate in aqueous solution, it is necessary to intentionally oxidize the Si(100) surface after cleaning to provide a hydrophilic surface for the mask solution. Unfortunately, this oxide layer complicates the subsequent dry etching step, because etching through the oxide and then etching into the underlying Si requires process adjustment mid-stream. Therefore, it is desirable to eliminate (or at least reduce the thickness of) this intenntional oxide layer from the process stream.

2.2. to carry out LE4 with the sample on the anode of the DC discharge;

in order to achieve greater control over the profile and the rate of the etch, we have relocated the sample to rest on the anode of the DC plasma reactor instead of allowing the sample to float to the plasma potential, as in our earlier work. This configuration greatly increases the

fraction of the discharge current arriving at the sample (which in turn increases the etch rate) and affords greater control over the energy of the incoming electrons.

2.3. to develop methods for stripping the mask after LE4;

after application to the Si(100) surface, the biomolecular template is coated with 1.2 nm of titanium metal, which is then oxidized. Consequently the nano-pattern is defined by a titania mask some 3.5 nm thick. After LE4, it is necessary to remove this mask by wet chemical methods, but without degrading the nano-pattern etched into the Si surface.

2.4. to deposit GaAs quantum dots on the nano-patterned substrate.

After the mask has been stripped, a few monolayers of GaAs will be deposited on the nano-patterned Si(100) substrate by Molecular Beam Epitaxy (MBE). The deposition temperature will be chosen high enough to ensure adequate surface mobility of the Ga and As ad-atoms but not so high as to "anneal out" the etched nano-pattern.

3. WORK PERFORMED: EXPERIMENTAL PROCEDURES AND RESULTS

3.1. Deposition of the biomolecular template directly on (hydrophobic) Si(100)surfaces

The biomolecular mask is derived from the two-dimensional protein crystals which form the surface layer (S-layer) of the archaebacterium *Sulfolobus acidocaldarius.* These crystals have an hexagonal array of pores 5 nm in diameter with a lattice constant of 22 nm. Figure 1 shows an Atomic Force Microscope (AFM) image of a typical protein crystal.

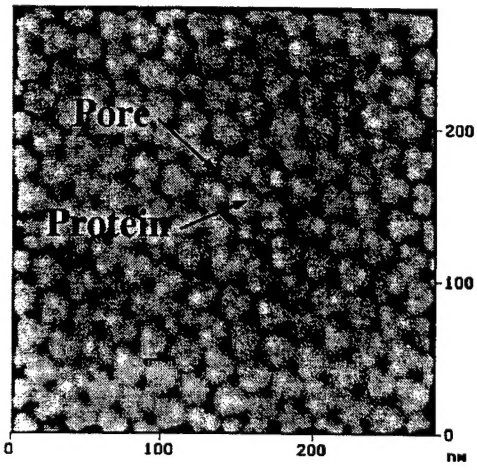

Figure 1. AFM image of an S-layer from *Sulfolobus acidocaldarius.* The S-layer is represented by the multiply-connected yellow area, and the pores are represented by red dots.

The AFM uses false color to represent height–tall features appear bright, short features appear dark. Therefore, in Fig. 1, the S-layer is represented by the multiply-connected yellow area, and the pores are represented by red dots. S-layers exist with a variety of lattice constants (~3 - 30 nm), different symmetries (i.e., square, hexagonal, oblique), and varying pore diameters (~0.2 - 10 nm).[2]

Typically, the biomolecular masks are applied to a substrate in a drop of water. In our previous work (See Reference 1), the freshly cleaned Si(100) wafer was intentionally oxidized to prepare a controlled, thin SiO_2 layer. This controlled native oxide layer is hydrophilic, allowing the water containing the biotemplates to wet the surface and create a very uniform concentration of biotemplates on the surface. This native SiO_2 layer, exposed in the open pores of the biomolecular mask, complicates the etching step because etching through the

oxide and then etching into the underlying Si-- using etch conditions that do not destroy the biomolecular mask--requires process adjustment mid-stream.

The obvious solution is to omit this intentional SiO_2 layer. This would be problematic because after dipping in HF as the final step in the initial cleaning process, the Si surface is extremely hydrophobic, preventing the water containing the biotemplates from wetting the surface. After considerable experimentation, we have circumvented this problem by adding a small amount (< 0.01 %) of Triton X-100, a common surfactant, to the biotemplate solution. This allows us to create nano-masked samples which are nearly oxide-free; these samples should show better quality and rate in the LE4 process.

Examination by X-ray Photoelectron Spectroscopy (XPS) demonstrates that our technique for applying the S-layers to a hydrophobic, oxide-free Si surface is working correctly. After application of S-layers, subsequent deposition of titanium (see following paragraphs), and confirmation by AFM that the S-layer pattern was in placed on the substrate, the XPS spectrum in Figure 2 was acquired from that sample.

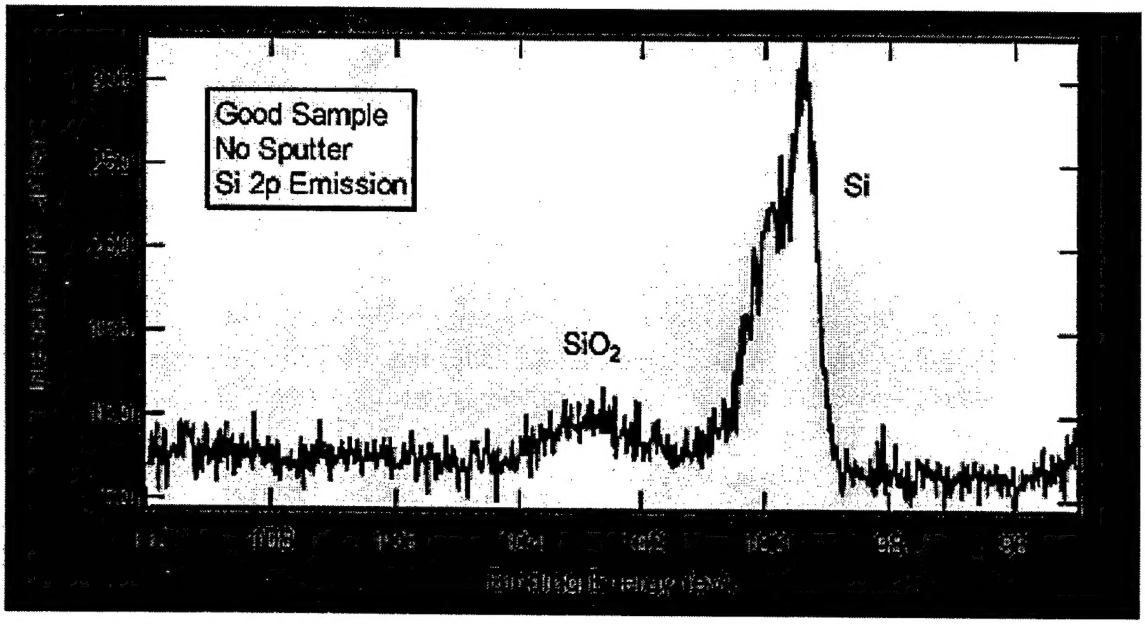

Figure 2. Spectrum from Ti-coated S-layers on Si (SiO_2 intentionally removed before S-layer application).

The strong Si(2p) peak near 99 eV is due to elemental Si, while the smaller Si(2p) peak near 103 eV is due to SiO_2. The relative heights of these two peaks suggests that there is still very little native oxide on the surface of the substrate after S-layer application and Ti deposition. This lack of native oxide should facilitate the LE4 process step.

In Figure 3 below, results achieved in etching samples masked by this new hydrophobic procedure are compared with those on samples masked by the original method. All results shown in figures thereafter were obtained from samples prepared by depositing the templates on freshly cleaned, hydrophobic Si(100) surfaces.

These deposited protein crystals are transformed into etch masks by coating them with a thin layer of titanium (Ti) deposited at an angle by electron beam evaporation. Upon exposure to air, the Ti oxidizes completely to titanium dioxide (TiO_2) forming a robust etch mask. Because the substrate surface in the pore sites of the S-layer is shadowed by the S-layer protein, the Ti is not deposited in those areas. Consequently, a hole is formed in the Ti layer at each pore site of the S-layer. Therefore, in a single step, the pattern of the S-layer is transferred to the Ti layer which ultimately becomes the TiO_2 etch mask. This massively parallel step simultaneously defines an entire array of nano-pores, avoiding entirely the slow steps that would be required to define such arrays by serial lithography.

The amount of titanium deposited, and thus the ultimate thickness of the mask, is limited by the need to avoid blocking the pores when the oxide forms. The titanium oxide thickness typically is measured to be 3.5 nm by AFM and confirmed by spectroscopic ellipsometry. The metallized pore diameter is ~6 nm. Because the TiO_2 mask is much thinner than standard masking materials used in microfabrication processes, it is susceptible to removal during standard ion-based dry etching. A much gentler dry etching process is required to transfer this pattern.

3.2. LE4 with the sample on the anode of the DC discharge

LE4 was developed to avoid the ion bombardment damage inflicted on the substrate by the standard ion-enhanced dry etching techniques in fabrication of semiconductor nanostructures. LE4 therefore is especially well suited for etching nanopatterns defined by thin or delicate mask materials. In LE4, electrons with kinetic energy 1 - 15 eV and chemically reactive species at thermal velocities are delivered simultaneously to the surface. These low-energy electrons impart negligible momentum to the surface and thereby avoid damage while enhancing the etch chemistry to give pattern transfer with controlled profiles. LE4 is accomplished either in ultrahigh vacuum (UHV) with separate beams of electrons and molecules[3] or in a DC plasma.[4] It has produced excellent anisotropy (vertical sidewalls) and smooth surfaces and maintained stoichiometry of compound semiconductor surfaces when etching Si,[4] GaAs,[5] and GaN.[6,7,8]

Systematic studies of LE4 have identified the process parameter space for damage free etching, with excellent anisotropy and surface morphology, of Si and GaAs in a hydrogen or chlorine DC discharge. Compared to RIE or ECR plasma etching, LE4 provides effective control of the energy of charged species bombarding the sample surface. At the anode of a DC discharge, the energy of electrons bombarding the sample surface is limited by the ionization potential of the process gas (usually 15 - 20 eV); this is substantially lower thaN the ion energy in a typical RIE process (200-300 eV). Eliminating the ion damage is critical in nanofabrication because the penetration depth of ion-induced damage (5-15 nm) is comparable to or even greater than the feature scale. Thus, LE4 is ideally suited for ultrasmall pattern transfer.

In our previous work on forming ordered arrays of Ti quantum dots (See Reference 1), the biomolecular template was deposited on oxidized (hydrophilic) Si(100) surfaces. During LE4, the templated sample was electrically isolated, and the potential of the sample was allowed to float to the natural potential of the plasma. We relied on the self-bias produced in the plasma to direct electrons to the surface so etching could occur. The samples were etched at a pressure of 60 mtorr H_2 and a discharge current of ~60 mA for 90 minutes.

In order to achieve greater control over the profile and the rate of etching the nanometer-scaled pattern, we sought to use the LE4 configuration that had produced excellent results on micrometer-scaled patterns (See References 4-8). In this configuration, the sample rests on the anode of the DC plasma reactor. This configuration greatly increases the fraction of the discharge current arriving at the sample (which in turn increases the etch rate) and affords greater control over the energy of the incoming electrons. We investigated etch times ranging from 5 - 60 minutes in Cl_2 and in H_2. We found that, in this anodic configuration, we could produce arrays of Ti dots similar to the earlier work after etching for only 15 minutes with a current of only 30 mA in H_2. The uniformity of the dots has improved when compared with our previously published results (Fig. 3).

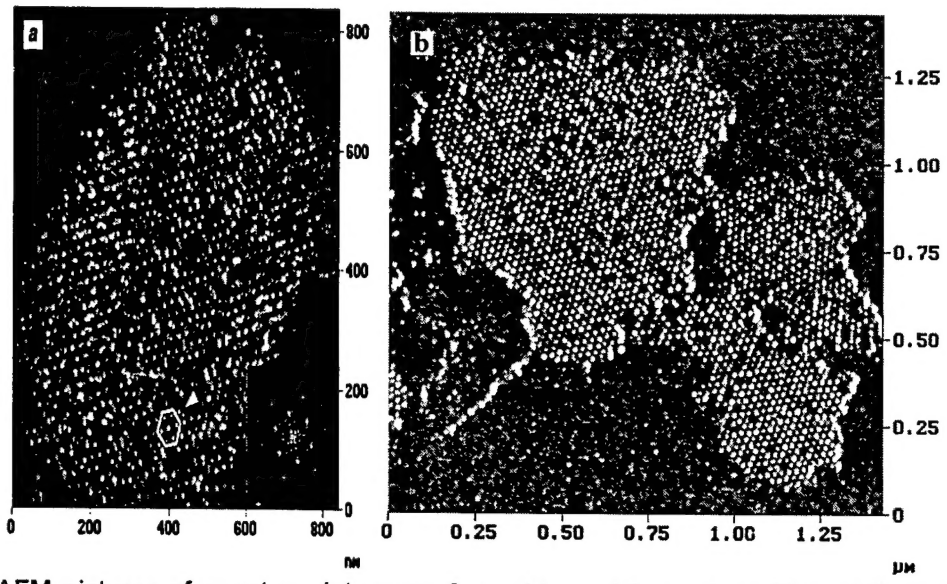

Figure 3. AFM pictures of quantum dot arrays formed by a 1.2 nm deposition of Ti onto a substrate nanopatterned with LE4 through a biomolecular mask. a) Substrate etched in floating mode. b) Substrate etched in anodic mode.

In Figure 3(b), the missing dots are caused by contamination present on the biotemplates before etching. Because our process for depositing the biotemplates on a hydrophobic substrate was new at this point, we had not yet optimized it and eliminated these contaminants. Despite these imperfections, it is clear that the dots are much more uniform when the substrates are etched in anodic mode.

Subsequent studies demonstrated that the contaminant is hydrophobic, and is therefore strongly attracted to the hydrophobic surface of the clean Si(100) wafer. High speed centrifugation failed to remove this material from the template solution, probably due to the small size of the particles (20 - 100 nm wide as viewed in the AFM). Dialysis significantly reduces the amount of this contamination in the protein crystal solutions, and increases the fidelity of the arrays as well as the uniformity of the dots in all the figures shown hereafter in this report.

Samples etched in Cl_2 for as little as 5 minutes appeared to have been over-etched. We will optimize the etch parameters for Cl_2 later on, when very rapid production of the nano-patterned substrates is required. Based on the results in Figure 2(b), we adopted anodic etching in DC hydrogen plasma as our baseline LE4 process for preparing nano-patterned substrates for the remaining exploratory work.

3.2.1. Preliminary Summary of LE4 Results.

Based on the results described to this point, we defined a very specific protocol for etching and evaluating nano-patterned substrates in preparation for growth of semiconductor quantum dot arrays:

1. Deposit S-layers from (dialyzed) solutions onto 8mm x 8 mm square pieces of Si(100) freshly cleaned and etched in aqueous HF solution.
2. Deposit 1.2 nm of Ti metal over the S-layers, and oxidize to form the titania etch mask.
3. Expose masked samples to anodic LE4 in pure hydrogen DC discharge at 60 mTorr total pressure and *ca.* 30 mA discharge current for 15 minutes.
4. After LE4, remove the titania mask by soaking the samples in 1:1 solutions of sulfuric acid in water at 130°C. Examine by AFM.
5. Cleave the stripped samples into two 4 mm x 4 mm pieces. Reserve one piece, and continue the evaluation with the second piece.
6. Expose the second piece to oxygen plasma for 4 minutes.
7. Deposit 1.2 nm of Ti metal on the oxidized piece.
8. Examine this piece by AFM. If Ti dots formed as in Figure 3(b), the etch is deemed successful, and the piece of the sample reserved at Step 5 can be safely used in further studies.

3.2.2. Reproducibility of Anodic LE4 for Nanostructure Arrays.

Despite our successes summarized to this point, we found it extremely difficult to obtain the etching results in Figure 3(b) on a regular basis, even when AFM examination of the templated samples before LE4 demonstrated that a high quality etch mask, free of protein contamination, had been prepared. We traced the reproducibility problems in anodic LE4 of these nano-patterned samples to three sources:

A. Instabilities in hydrogen DC plasma with very small anodes;
B. Redeposition of amorphous Si from decomposition of SiH_4 etch products;
C. Interference by small amounts of organic contaminants in the LE4 reactor.

Elimination of each of these sources will be described in turn. Elimination of *A* and *B* requires careful attention to nature of the DC discharge in the process gas, and to interactions of the thermodynamics of the particular etching reaction with the properties of the LE4 reactor. Elimination of C is somewhat mundane, but is included here to illustrate the fact that contamination that would be entirely acceptable in etching micrometer-scaled structures can completely defeat the etching of these nanometer-scaled arrays.

3.2.3. Enhanced Stability of Hydrogen DC Plasmas.

It has been recognized in the literature of DC glow discharges that pure hydrogen is more difficult to ionize than the inert gases, because it lacks metastable states between the ground state and the ionization threshold. [9] Thus, ionization in the pure hydrogen glow is produced only by collisions with electrons that have sufficient energy to reach the ionization threshold in a single collision. By contrast, the inert gases have much higher effective ionization coefficients because their numerous metastable states M* can produce ions by colliding with each other as in

(1) $$2\,He^* \rightarrow He^+ + e^- + He$$

or by colliding with ground state neutral atoms of a different gas as in

(2) $$Ne^* + Ar \rightarrow Ar^+ + e^- + Ne$$

The second equation is the basis of the so-called "Penning effect" in which specially chosen gas mixtures in DC glow discharges show very high effective ionization efficiency, and consequently high discharge current density, at unusually low values of the characteristic parameter X = electric field/pressure. Penning mixtures see practical applications in a wide variety of gaseous electronic devices.

Since we had already successfully etched Si samples in pure hydrogen DC plasma in this project, our goal in choosing an additive to the discharge gas was more to increase current density than to reduce electron energy. Consequently, we selected argon, the inert gas whose ionization potential (15.6 eV) was closes to that of molecular hydrogen (15.4 eV). Indeed, argon does not show the Penning effect with hydrogen, since the energy value of the argon metastable state is only 12.5 eV. Moreover, hydrogen molecules can quench some of the argon metastable atoms through collisions to produce ground state atoms, thereby reducing the number of ionization events described by the first equation below the number that would occur in pure argon. Nonetheless, we have observed that 50% mixtures of argon and hydrogen in a DC glow will sustain a much higher discharge current at a given discharge voltage, and operate with much greater stability, than will a discharge in pure hydrogen.

Consequently, we switched from pure hydrogen plasma to 50-50 mixtures of hydrogen and argon in the present approach. Operating on these mixtures at pressures of 82-84 milliTorr and total flow rates of 13-14 sccm, our LE4 reactor gave extremely stable and reproducible plasmas with discharge current as high as 220 mA at 2.5 kV. The current and voltage could be adjusted readily to lower values, maintaining both the stability and the reproducibility of the plasma. These conditions have been selected as the baseline LE4 process for the remainder of this project. Examples of successful etching will be illustrated below, after the problem of re-deposition of amorphous Si on the sample during LE4 has been described and eliminated.

3.2.4. Elimination of Silicon Re-deposition on Sample during LE4.

Even after the LE4 process was improved by switching to 50-50 mixtures of hydrogen and argon, it still lacked sufficient reproducibility, due to the occasional appearance of deposited particulate matter that sometimes forestalled the etching process entirely by covering the S-layers, and on other times impeded the etching process by partially blocking some of the holes in

the S-layers. This was traced to the re-deposition of Si due to decomposition of the volatile etch product silane in the plasma above the sample, and has been eliminated by the methods described in the following paragraphs.

Figure 4 shows the AFM image of a typical sample on which particulates appeared after the LE4 process.

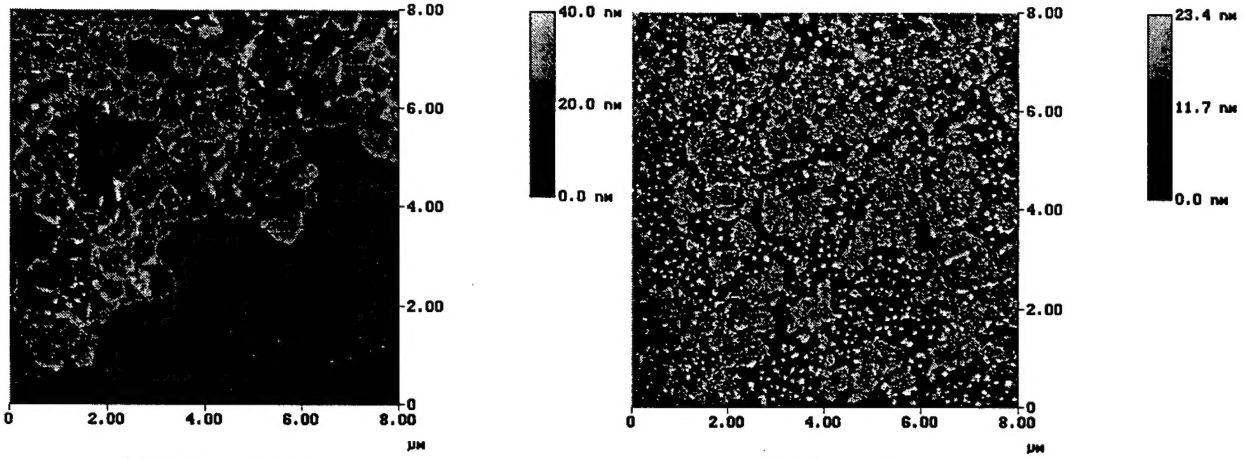

(a) Before etching **(b) After etching**

Figure 4. Particulate Material deposited during LE4 Process.

Given the small size of these particles, we were unable to perform definitive chemical analysis. However, we hypothesized that they were re-deposited Si, since we had observed silicon re-deposition on micrometer-scaled features during LE4 of Si in hydrogen plasma in one of our earliest studies of the LE4 process, and demonstrated that it was caused by electron-induced decomposition of the SiH_4 etch product.[10] Relying on results established in this earlier work for controlling the energy and current of electrons by adding noble gases to the hydrogen plasma, partly motivated our switch from pure hydrogen plasma to 50-50 mixtures of hydrogen and argon as descraibed in the previous section. Etching under these conditions reduced particulate deposition, but did not eliminate it completely.

Further investigation revealed that Si re-deposition during etching in a hydrogen plasma depends on temperature, as well as on electron energy, in a manner that can be rationalized by chemical thermodynamics. The change in standard Gibbs free energy at 298K for the etching (volatilization) reaction

(3) $$Si_{(s)} + 2\ H_{2(g)} \leftrightarrow SiH_{4(g)}$$

is $\Delta G° = +60\ kJ \cdot mol^{-1}$; consequently, this reaction is not spontaneous. The free energy change becomes even more positive at high temperatures. Thus, the decomposition of silane is more favorable thermodynamically than its formation by reaction (1). But, if the hydrogen molecules are first dissociated into hydrogen atoms so the reaction becomes

(4) $$Si_{(s)} + 4\ H_{(g)} \leftrightarrow SiH_{4(g)}$$

the standard free energy change at 298 becomes $\Delta G° = -756$ kJ·mol^{-1} which has a slight tendency for spontaneity. Thus the etching reaction is spontaneous in a hydrogen plasma, where hydrogen molecules are dissociated into atoms by the energy of the plasma. At higher temperatures, the free energy change for reaction (4) becomes progressively less negative, leading to a progressively smaller equilibrium constant for reaction (4). Consequently, despite the substantial flow rates in a plasma reactor, this reaction appears to remain in quasi-equilibrium, in which the presence of SiH_4 not only impedes the progress of reaction (4) but can lead to re-deposition of solid Si on the etching sample by the reverse of reaction (3). To forestall this effect, we place additional Si wafers (dubbed the "witness wafers") near to and downstream from the etching sample in the LE4 reactor, and maintain them at temperatures higher than the etching sample. This higher temperature increases the equilibrium constant for the reverse of reaction (3), and favors re-deposition of Si on the witness wafers rather than on the etching sample. This same phenomenon had been observed earlier by Veprek and his collaborators in their studies of the hydrogen plasma-assisted chemical vapor transport of silicon to form H-doped micro-crystalline Si thin films for photovoltaic applications.[11 12] In Veprek's work, H atoms generated in the plasma removed Si atoms from "source" wafers by reaction (4), then deposited amorphous and micro-crystalline Si films on a hotter "substrate" Si wafer downstream in the reactor by the reverse of reaction (3).

3.2.5. Final Summary of LE4 Results.

These studies described in the previous two sections have led us to the following set of etching parameters for LE4 of Si(100) surfaces:

Table 1: Standard Etch Parameters

Gas composition:	50-50 Ar and Hydrogen
Total pressure:	84.4 mTorr
T (sample):	70 C
T (wit.waf.):	333 C
Voltage:	1.7 kV
Current density:	130 mA/cm^2 (65 mA over sample area 0.5 cm^2)
Etch time:	50 min

which produce etched samples that are mirror-smooth with no sign of discoloration or deposition. Immediately after LE4, AFM images show no evidence of particulates. When the titania-S-layer mask is stripped away in hot sulfuric acid solution, the AFM images of the etched surface is shown in Figure 5:

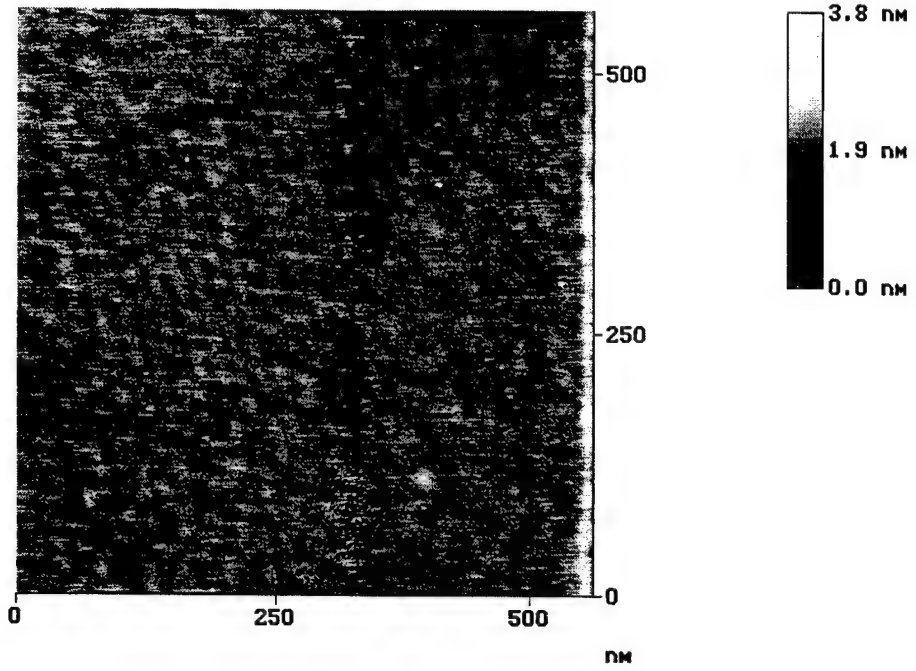

Figure 5. Array of nano-holes etched in Si(100) substrate using conditions in Table 1.

The diagonal feature running lower left to upper right is the hexagonal array of holes etched in the region covered by an S-layer fragment; the higher plateaus in the upper left corner and on the right-hand side represent areas of the Si wafer that were protected by the un-interrupted titania mask, and consequently were not etched. Although the conditions in Table 1 do not represent a fully optimized LE4 process, they lead in a highly reproducible way to etched surfaces such as that shown in Figure 5.

We are now able routinely to prepare surfaces such as that in Figure 5 for studying formation of quantum dot arrays upon deposition of ad-atoms.

3.2.6. Epilogue: Effects of Organic Vapor Contaminant in the LE4 Chamber

One annoying and time-consuming side issue interfered with achieving the reliable baseline LE4 results summarized in Section 3.2.5. At one point during Month 4, all attempts to achieve LE4 failed. All the template-masked samples processed in the LE4 system were discolored as if a thin film had been deposited on them, and none of them etched.

To identify the deposited film definitively, we performed XPS. To serve as reference, we obtained a spectrum from a sample with Ti-coated S-layer crystals (confirmed by AFM) that had not been inside the LE4 chamber. The spectrum is shown in Figure 6.

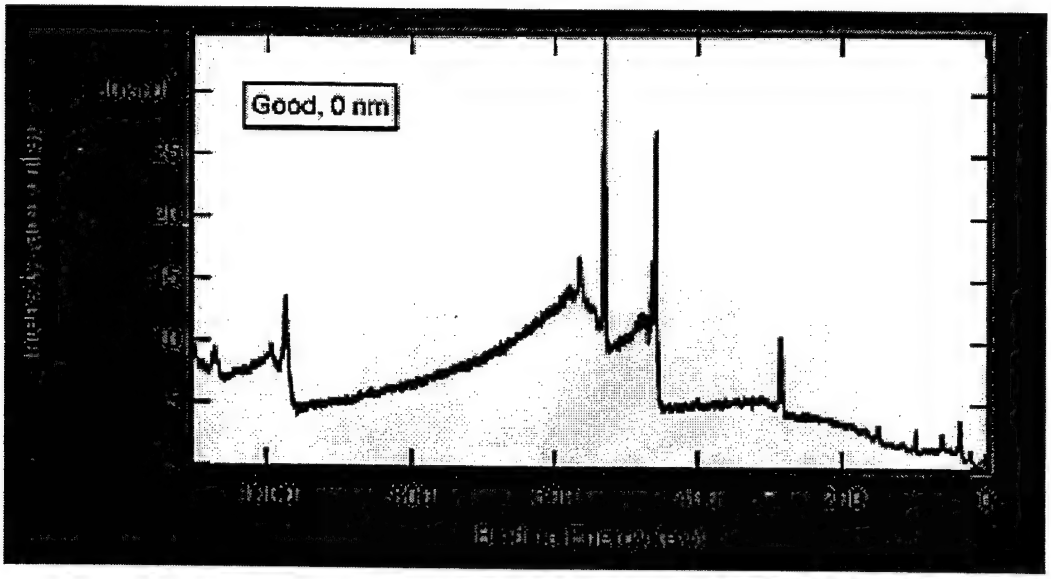

Figure 6. Baseline XPS spectrum from a sample that had never been inside the LE4 chamber.

All the peaks were consistent with Ti-coated S-layer on Si. Next, the spectrum shown in Figure 7 was acquired from the (blue) discolored area on one of the samples described above.

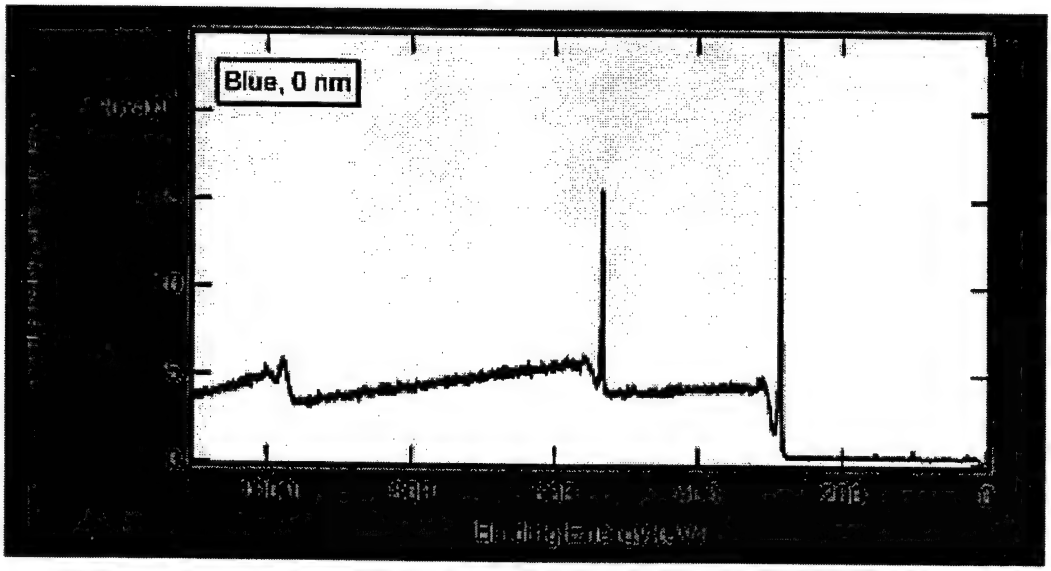

Figure 7. Survey spectrum from the discolored area of an LE4-etched sample.

Figure 7 shows that the discolored area is composed of carbon [C(1s) with BE near 274 eV] and oxygen [O(1s) with BE near 532 eV]. To get some indication of the depth of this discolored layer, we sputtered the sample with Ar ions and then acquired the spectrum in Figure 8.

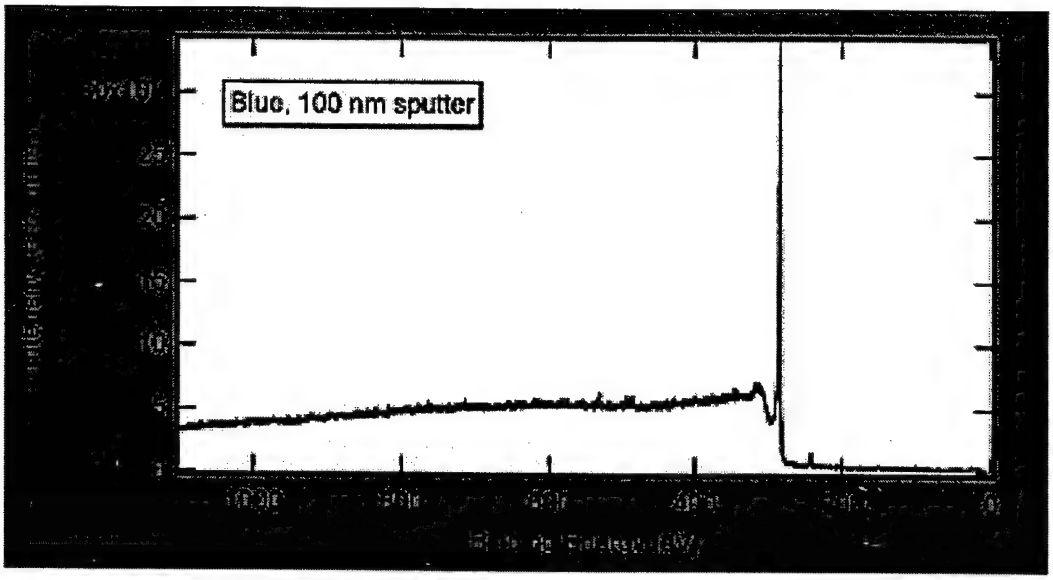

Figure 8. Survey spectrum from the discolored area after sputtering to a depth of 100 nm.

The composition of the surface film at this depth is primarily carbon, and it is sufficiently think to mask photoemission from the underlying S-layers and substrate.

The only reasonable explanation for depositing a carbon-containing film instead of etching is that an organic vapor contaminant in the LE4 chamber undergoes "plasma polymerization" under electron impact on the surface of the sample. This polymerized layer prevents etching from occurring at the pore sites of the S-layer.

The silver paste used to improve electrical contact between sample and anode was shown to be the source of this problem. This conducting adhesive is a standard product routinely used to attach samples to the stage during Scanning Electron Microscopy, and we had used it routinely during our earlier LE4 work on micrometer-scaled Si surfaces. The organic matrix in which the colloidal silver is suspended produced sufficient vapor to cause film deposition during etching. This problem appeared at Month 4 in our program and not earlier because we had then recently switched to a new brand of silver paste for which the outgassing specifications proved unreliable. The reactor was completely dis-assembled and cleaned to remove any residual organic impurities. To eliminate the silver paste entirely and still obtain good electrical and thermal contact between sample and stage, we now deposit a layer of 10 nm of tantalum on the backside of the substrate of each sample, then attach the sample to the stage with a soft indium foil. Since adopting this procedure, we have had no further occurrences of extraneous film deposition during etching.

3.3 Stripping the Template-Generated Mask after LE4

The biomolecular mask derived from S-layers is converted into an inorganic template of titanium oxide, which cannot be removed by the standard solvents used to remove photoresist in microfabrication processes. After considerable experimentation, we observed that this mask could be removed by soaking the samples in 1:1 solutions of sulfuric acid in water at 130°C with ultrasonic agitation. Examination of stripped samples by XPS shows no trace of titanium. Examination by AFM shows that the nano-array of holes has been transferred to the Si(100)

substrate. An example of the results at this point--corresponding to Step 4 in the evaluation protocol defined in Section 3.2.1-- is shown in Figure 5 above.

The stripping process is a delicate operation, since it must remove the titania mask without degrading the underlying etched nano-array. Our procedure is adapted from the first step (by omitting the hydrogen peroxide) of the standard wet cleaning processes for Si(100), which is aimed primarily at removal of transition metal impurities and carbon. Even without the peroxide, this method is likely to produce limited oxidation of the nano-patterned surface. To remove this, the samples are given a quick dip in 5% HF aqueous solution after stripping, and again examined by AFM. The patterns as shown in Figure 5 are intact at this point, and we proceed with attempts to grow quantum dot arrays on the nano-patterned substrate.

3.4 Growth of GaAs Quantum Dot Arrays on Nano-patterned Si(100) Substrates.

A total of 6 Si(100) samples patterned from S-layers using LE4 in DC hydrogen plasma, with etch results comparable to those in Figure 5, were exposed to GaAs growth by Molecular Beam Epitaxy (MBE) in the laboratory of Dr. Kris Bertness at NIST in Boulder, CO. The range of growth conditions explored is summarized in Table 2.

Table 2: MBE Conditions for GaAs Growth on Si nanopatterned substrates

Samp. No.	Growth Temp[C]	Growth rate[ML/s]	Outgas Temp[C]	Comments
B241	400	0.302	570	
B250	500	0.302	600	Arsenic pulse, 1 min wait before run start
B251	450	0.302	550	Arsenic pulse, 1.5 min wait before run start
105	500	0.487	600	
110	500	0.487	600	
CTRL	500	0.487	600	

Each sample was outgassed at the temperature shown before the start of the growth run. Each run comprised six growth cycles alternating between Ga and As, with the Ga coverage about 1 ML per pulse. The arsenic time open is half as long for B250 and B251 as it was for B241. Figure 9 and Figure 10 show AFM images of two of these samples after GaAs growth. Note that the scan ranges in these figures are substantially larger than that in Figure 5, in order to examine several S-layer regions for ordered arrays of GaAs dots on the nano-patterned surfaces.

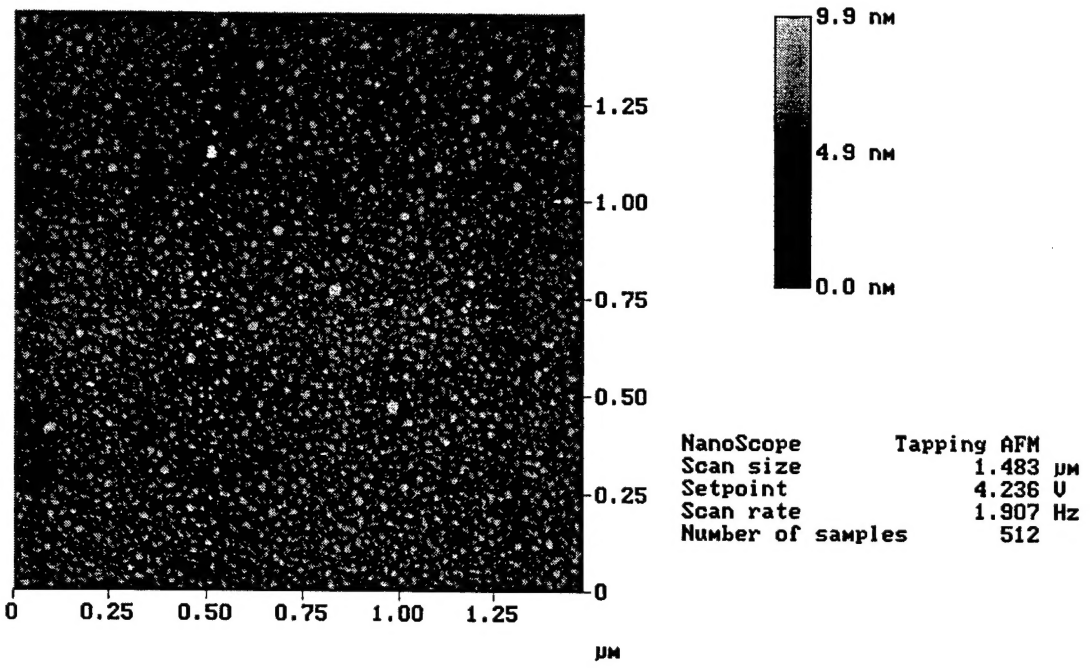

Figure 9. AFM of Nano-patterned Sample 105 after MBE Growth of GaAs.

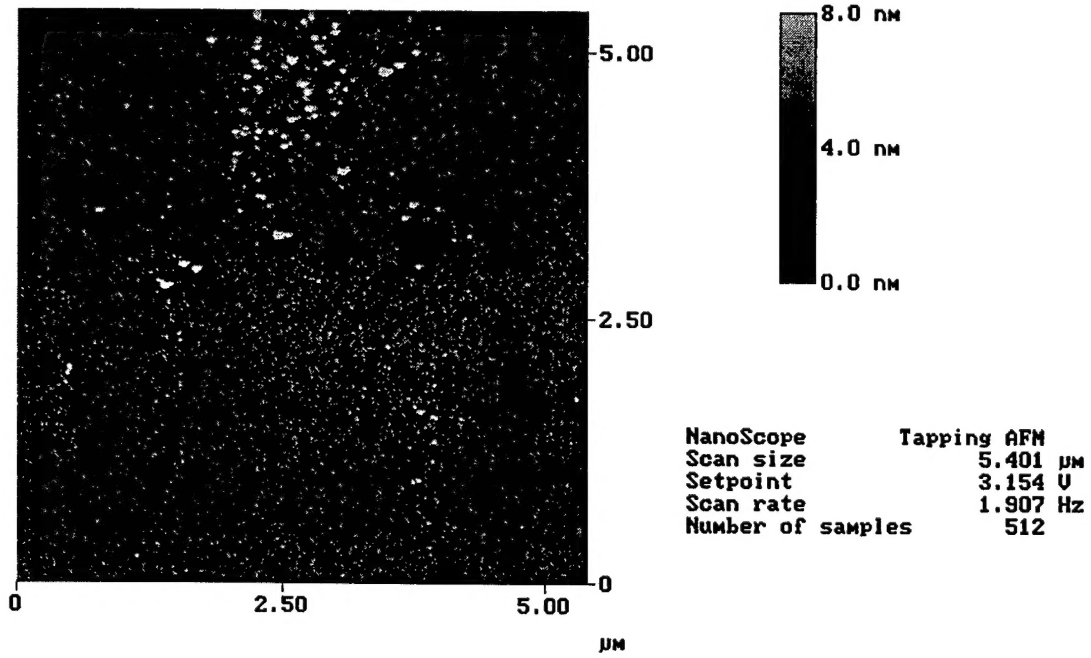

Figure 10. AFM of Nano-patterned Sample 110 after MBE Growth of GaAs.

Both these figures show dots of GaAs, but they are randomly distributed over the surface rather than ordered over the arrays of nano-holes that were placed in the surface before growth. One clue to this behaviour comes from the observation that the RHEED (Reflected High Energy Electron Diffraction) patterns obtained from the surfaces before GaAs growth was started were completely diffuse, despite the presence of the nano-patterns as confirmed by AFM. This suggests that the nano-patterned surface was substantially oxidized, even in the nano-holes, and

therefore appeared to the grown GaAs more like a flat oxidized Si surface than a nano-patterned clean (or hydroden terminated) Si surface. For comparison, Figure 11 shows the AFM of similar GaAs growth runs on a "control" surface that was a non-patterned, blank chip of Si(100).

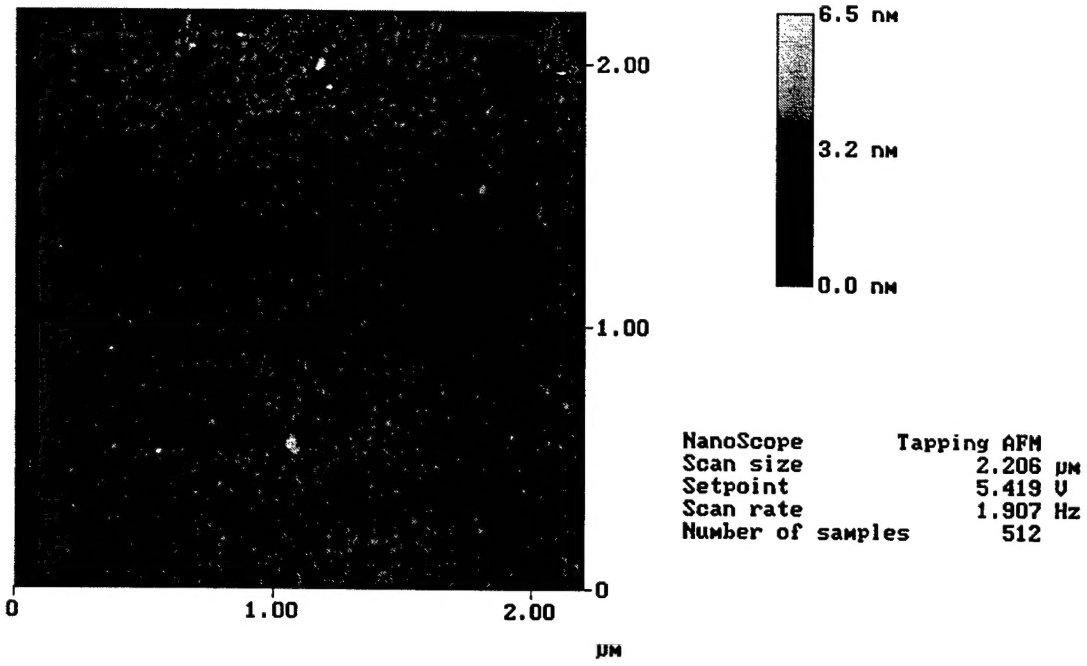

Figure 11. AFM of Control sample (blank piece of Si) after GaAs MBE.

The results are indistinguishable from those in Figure 9 and Figure 10, and confirm that the morphology of the deposited GaAs is dominated by the oxidized Si surface rather than by the underlying nano-patterns in the Si(100) surface.

Clearly, it will be necessary to perform surface characterization of the nano-patterned surfaces shown in Figure 5 and to develop a suitable cleaning procedure—perhaps a combination of gentle wet etching and thermal desorption of oxide in ultrahigh vacuum just before the start of GaAs growth—in order to reveal the influence of the nano-pattern on GaAs dot growth.

5. TECHNICAL FEASIBILITY OF THE APPROACH

Our approach to forming ordered arrays of semiconductor quantum dots on a substrate relies on four key steps:

- Attach S-layer templates to a clean, hydrophobic Si(100) substrate and convert them to a titania etch mask;
- Transfer the pattern into the substrate using LE4;
- Strip the titania mask from the sample after LE4, and confirm that the nano-array has been defined in the substrate;
- Grow one semiconductor quantum dot in each hole of the array to form an ordered array of quantum dots.

The results achieved in this Phase I project demonstrate that we have reliable methods for attaching the S-layer biomolecular templates to the Si(100) substrate and converting them into a reasonably robust etch mask. We also have reliable methods for transferring this pattern into the substrate by LE4 in the anodic configuration, using 50-50 mixtures of argon and hydrogen. Developing this anodic LE4 process for the nano-pattern was in fact the central effort in Phase I. We also have a method for stripping the mask, and we can confirm that the nano-array is in place after stripping.

However, we do not yet have firm control over the extent of oxidation of this nano-patterned surface, and the influence of this (presumed) oxide layer on subsequent growth of quantum dots. Accordingly, Step 3 will be the central focus of our Phase I Option project, in which we will develop a reliable stripping process to enable systematic studies of quantum dot deposition conditions, and their dependence on characteristics of the etched nano-array, in Phase II. Work on this critical Step 3 has already started in the Phase I Option that was recently authorized. Progress in that direction will be described in the first monthly report in the Phase I Option period.

---

[1] T. A. Winningham, H. P. Gillis, D. A. Choutov, K. P. Martin, J. T. Moore, and K. Douglas, Surf. Sci. **406**, 221 (1998).

[2] U.B. Sleytr and P. Messner, Ann. Rev. Microbiol. **37**, 311 (1983).

[3] H.P. Gillis, J.L. Clemons, and J.P. Chamberlain, J. Vac. Sci. Technol. **B10,** 2729 (1992).

[4] H.P. Gillis, D.A. Choutov, P.A. Steiner IV, J.D. Piper, J.H. Crouch, P.M. Dove, and K.P. Martin, Appl. Phys. Lett. **66,** 2475 (1995).

[5] H.P. Gillis, D.A. Choutov, K.P. Martin, and Li Song, Appl. Phys. Lett. **68,** 2255 (1996).

[6] H.P. Gillis, D.A. Choutov, K.P. Martin, S.J. Pearton, and C.R. Abernathy, J. Electrochem. Soc. **143,** L251 (1996).

[7] H.P. Gillis, D.A. Choutov, and K.P. Martin, Jour. of Materials **48,** 50 (1996).

[8] H.P. Gillis, D.A. Choutov, K.P. Martin, M.D. Bremser, and R.F. Davis, J. Electr. Mat. **26,** 301(1997).

[9] J.R. Acton and J.D. Swift, Cold Cathode Discharge Tubes, Academic Press, New York, NY. 1963. Chapter 12

[10] H.P. Gillis, D.A. Choutov, P.A. Steiner IV, J.D. Piper, J.H. Crouch, P.M. Dove, and K.P. Martin, "Low Energy Electron Enhanced Etching of Si(100) in Hydrogen/Helium DC Plasma," Appl. Phys. Lett. **66,** 2475 (1995).

[11] S. Veprek et al, "Parameters Controlling the Deposition of Amorphous and Microcrystalline Silicon in Si/H Discharge Plasmas," J. de Physique (Paris) **42-C4**, 251 (1981).

[12] S. Veprek et al, "Highlights of Preparative Solid State chemistry in Low Pressure Plasmas," Pure & Appl. Chem. **54**, 1197 (1982).